

D. Roeland Boer,<sup>a</sup> Axel Müller,<sup>a‡</sup>  
Susanne Fetzner,<sup>b</sup> David J.  
Lowe<sup>c</sup> and Maria João Romão<sup>a\*</sup>

<sup>a</sup>REQUIMTE/CQFB, Departamento de Química, Faculdade de Ciências e Tecnologia, Universidade Nova de Lisboa, 2829-516 Caparica, Portugal, <sup>b</sup>Westfälische Wilhelms-Universität Münster, Institut für Molekulare Mikrobiologie und Biotechnologie, Corrensstrasse 3, D-48149 Münster, Germany, and <sup>c</sup>Biological Chemistry Department, John Innes Centre, Colney, Norwich NR4 7UH, England

‡ Current address: Structural Biology Laboratory, Department Of Chemistry, University of York, Heslington, York YO10 5YW, England.

Correspondence e-mail: mromao@dq.fct.unl.pt

Received 27 October 2004  
Accepted 3 December 2004  
Online 24 December 2004



© 2005 International Union of Crystallography  
All rights reserved

## On the purification and preliminary crystallographic analysis of isoquinoline 1-oxidoreductase from *Brevundimonas diminuta* 7

Isoquinoline 1-oxidoreductase (IOR) from *Brevundimonas diminuta* is a mononuclear molybdoenzyme of the xanthine-dehydrogenase family of proteins and catalyzes the conversion of isoquinoline to isoquinoline-1-one. Its primary sequence and behaviour, specifically in its substrate specificity and lipophilicity, differ from other members of the family. A crystal structure of the enzyme is expected to provide an explanation for these differences. This paper describes the crystallization and preliminary X-ray diffraction experiments as well as an optimized purification protocol for IOR. Crystallization of IOR was achieved using two different crystallization buffers. Streak-seeding and cross-linking were essential to obtain well diffracting crystals. Suitable cryo-conditions were found and a structure solution was obtained by molecular replacement. However, phases need to be improved in order to obtain a more interpretable electron-density map.

### 1. Introduction

The molybdopterin-dependent enzyme xanthine dehydrogenase (XDH) has been widely studied owing to its pathogenic role in post-ischaemia reperfusion injury, acting as a source of reactive oxygen species (Harrison, 2002), and for its involvement in gout (Monu & Pope, 2004). The enzyme is a member of the mononuclear molybdenum family of proteins that have been grouped into three sub-families (Hille, 1996), one of which includes XDH and related enzymes. A number of crystal structures of proteins from the XDH family are now available, including the aldehyde dehydrogenases from *Desulfovibrio gigas* (MOP; Romao *et al.*, 1995; Rebelo *et al.*, 2001) and *D. desulfuricans* (MOD; Rebelo *et al.*, 2000), xanthine oxidase/dehydrogenases from bovine milk (Enroth *et al.*, 2000) and *Rhodobacter capsulatus* (Truglio *et al.*, 2002) and quinoline 2-oxidoreductase (QOR) from *Pseudomonas putida* 86 (Bonin *et al.*, 2004). In addition, the structure of the closely related CO dehydrogenase from *Oligotropha carboxidovorans* (Dobbek *et al.*, 1999, 2002) has been solved. The latter is the only enzyme of the XDH family solved to real atomic resolution (1.1 Å; Dobbek *et al.*, 2002). The enzymes of this family consist of a large subunit or domain, which contains a mononuclear Mo at the active site that is bound to a molybdopterin cofactor through a dithiolene moiety, and a small subunit or domain containing two [2Fe–2S] clusters. For some enzymes of this family, including XDH, QOR and CODH, the primary sequence includes another domain containing an FAD molecule that acts as a transient electron acceptor. The Mb atom in the active site has been shown to be pentavalently coordinated, being bound to the two sulfurs of the dithiolene moiety, an oxo and a sulfido ligand and an OH<sup>−</sup> ion or H<sub>2</sub>O molecule, although the active-site configuration of CODH contains an additional Cu atom. The crystal structures and extensive electron paramagnetic resonance (EPR; Hille, 1996) and extended X-ray absorption fine structure (EXAFS) studies (Cramer *et al.*, 1984; Bordas *et al.*, 1979) have greatly improved the understanding of the mechanism and function of this class of proteins. However, questions about details of the mechanism and substrate specificity or rather lack of substrate specificity remain unanswered. For example, the position of the sulfido ligand in the active site remains uncertain. It has been found in the equatorial position in bovine milk XDH (Okamoto *et al.*, 2004) and in QOR

(Bonin *et al.*, 2004), but resulfuration of MOP resulted in an active-site geometry with the S atom in the apical position (Huber *et al.*, 1996), whereas the crystal structure (Rebello *et al.*, 2001) suggests there is an oxo ligand instead (desulfo form). The structure of isoquinoline 1-oxidoreductase (IOR) from *Brevundimonas diminuta* 7, another member of the XDH family, is expected to contribute to the general understanding of these enzymes. In addition, IOR deserves crystallographic characterization because it is in several ways an outlier in the XDH family, as described below.

IOR is a heterodimeric protein that catalyses the first step of isoquinoline degradation (Fig. 1). It consists of two subunits, one of 80 kDa containing the Mo active centre and one of 16 kDa containing the two [2Fe–2S] clusters (Lehmann *et al.*, 1994). There are three remarkable differences between IOR and other members of the XDH family. Firstly, a sequence comparison of members within the family (Lehmann *et al.*, 1994, 1995) shows that the N-terminal part of the catalytic subunit of IOR, which consists of residues 39–113 (domain A), aligns well with an amino-acid stretch closer to the C-terminus of XDH. As a consequence, the sequence identity between the large subunit of IOR and corresponding units of other members of the XDH family is lower than the identity within those members. Secondly, the enzyme has a persistent ‘very rapid’ signal as determined by EPR spectroscopy, which is generally associated with an enzyme-bound catalytic intermediate (Canne *et al.*, 1999). This indicates that in the absence of an electron acceptor the catalytic cycle cannot be completed and substrate remains bound to the Mo atom. Finally, the protein appears to be very hydrophobic, an observation based on the fact that the protein crystallized in a screening condition designed for membrane proteins and also on its high affinity for hydrophobic resins employed in the purification. Hydrophobicity is a characteristic that has not been reported for other members of the family.

The purification and characterization of IOR has been described previously (Lehmann *et al.*, 1994) and involves heat-precipitation, hydrophobic interaction, cation-exchange and size-exclusion chromatography. However, attempts to reproduce the published purification protocol were unsuccessful. For unknown reasons, in some cases the protein was lost during the hydrophobic interaction chromatography (HIC) step. This problem was encountered previously (personal communication by SF) and depended on the cell culture used in the purification. The purification protocol was therefore reconsidered and different methods were tried in order to improve it. However, the choice of purification methods was severely restricted by the hydrophobic nature of the IOR, its instability at low pH and its complete loss of activity when subject to anion-exchange chromatographic methods. In this paper, we describe our efforts towards purification and crystallization of IOR. We report preliminary X-ray analysis and derivatization of the crystals using arsenite inactivation of the molybdenum active site (Boer *et al.*, 2004).

## 2. Experimental

### 2.1. Protein purification

Chemicals were ordered from Merck (Darmstadt, Germany) unless specified otherwise. Cells were grown as described previously (Lehmann *et al.*, 1994). Cells were lysed using an Emulsiflex-C5 French Press from Avestin (Canada) at ~100 MPa in three passes. Isoquinoline 1-oxidoreductase activity was determined by formation of INT-formazan (Lehmann *et al.*, 1994). Heat precipitation was performed at 328 K for 10 min. Triton X-100 precipitation was performed by adding pure Triton X-100 to the protein solution to a

final concentration of 1.5% (v/v). All column resin materials and hardware were from Amersham Pharmacia Biotech (Sweden) unless otherwise stated. All purification steps were performed on an Amersham HPLC containing UV-900, P-900 and Frac-900 units coupled to a PC running *Unicorn* software v.3.21.02. All steps were performed at 277 K. Hydrophobic interaction was performed using phenyl Sepharose 6 FF resin. Two cation-exchange columns were used: a hand-packed SQ Sepharose Fast Flow resin and a Resource 15S 1 ml prepacked column. Gel chromatography was performed on a pre-packed Superdex 200 column (60 cm). SDS-PAGE was performed using 10% separating gel (Schägger & von Jagow, 1987). Protein purity was determined using specific activity measurements and protein concentration was assessed by the Lowry method (Lowry *et al.*, 1951). The pure samples from the gel-chromatography column were combined and the buffer was replaced with 10 mM Tris–HCl pH 8.5 using iterative concentrating steps through centrifugation over a Millipore/Amicon YM-10 microcon with 10 kDa cutoff followed by dilution steps with the new buffer. The protein sample was subsequently concentrated to 20 mg ml<sup>-1</sup>. The purified protein samples were divided into 25 µl aliquots and stored at 193 K.

### 2.2. Crystallization

Suitable crystallization conditions were screened at 277 and 293 K using the hanging-drop vapour-diffusion method and the sparse-matrix-based Hampton Research Crystal Screens 1 and 2 as well as the Memstart membrane protein screen of Molecular Dimensions Inc. Two conditions of the Memstart screen were found to yield crystals at 293 K, the first containing 0.1 M NaCl, 100 mM HEPES pH 7.5, 10% PEG 4000 (crystallization buffer A) and the second 100 mM Tris–HCl pH 8.5, 12.5% PEG 8000 (crystallization buffer B1). Subsequent optimization experiments were performed by varying the pH in the range 6.5–9.0 (in steps of 0.5, using appropriate buffers for each pH) against the precipitant concentration (8–13% for buffer A, 10–15% for buffer B1) at both 277 and 293 K. Optimal conditions were found to correspond to the initial conditions identified in the screens. Hampton Additive Screens were applied in order to improve the morphology of the crystals grown in buffer B1. A 10 mM concentration of BaCl<sub>2</sub> gave the required improvement. The optimized crystallization conditions were based on the hanging-drop vapour-diffusion method at a temperature of 293 K using either crystallization buffer A or a buffer containing 10 mM BaCl<sub>2</sub> (Sigma-Aldrich), 100 mM Tris–HCl pH 8.5, 12.5% PEG 8000 (crystallization buffer B2) using a protein concentration of 20 mg ml<sup>-1</sup>. Streak-seeding was often used to induce crystallization and was performed with either cleaned rat whiskers or human eyelashes. Crystals appeared within hours and reached maximum dimensions after one week. A harvesting buffer containing 0.1 M NaCl, 100 mM HEPES pH 7.5, 12.5% PEG 4000 or 10 mM BaCl<sub>2</sub>, 100 mM Tris–HCl pH 8.5 and 15% PEG 8000 for buffers A and B2, respectively, was added to the drop containing the crystals after maximum size had been reached. Cross-linking was performed using the harvesting buffer

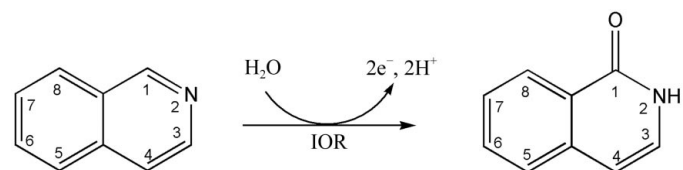


**Figure 1**  
Reaction scheme of the conversion of isoquinoline to isoquinoline-1-one, catalyzed by isoquinoline 1-oxidoreductase (IOR).

enriched with 1% glutaraldehyde or by simultaneous growth of IOR with betaine (carboxymethyltrimethylammonium) monohydrate at 10 mM initial concentration. Crystals were mounted using a cryoprotectant solution containing 30% PEG 4000 added to the appropriate harvesting buffer.

### 2.3. X-ray diffraction experiments

Diffraction experiments were carried out at the European Synchrotron Radiation Facility (ESRF) in Grenoble (France). A native data set was measured on a crystal grown in crystallization buffer *A* on beamline BM30A. Diffraction data were collected at 100 K at a wavelength of 0.976 Å to a maximum resolution of 2.5 Å. A two-wavelength MAD data set at the absorption *K* edge of Fe was measured on the ID29 beamline on native crystals grown in crystallization buffer *B2*. Crystals grown in buffer *B2* were soaked for 1 h in 10 mM NaAsO<sub>2</sub> to achieve inactivation of the protein by ligation of [AsO<sub>3</sub>]<sup>−</sup> to Mo (Boer *et al.*, 2004). A data set at the absorption *K* edge of As was measured at 100 K on the ID14-EH4 beamline. The data are summarized in Table 1. The native data were processed using the *DENZO/SCALEPACK* package (Otwinowski & Minor, 1997); all other data were processed using the *XDS* program (Kabsch, 1993).

### 3. Results and discussion

As mentioned previously, the reported purification protocol (Lehmann *et al.*, 1994) includes heat precipitation, hydrophobic interaction, cation-exchange and size-exclusion chromatography, with a yield of 68%. However, we were unable to reproduce the reported yield because of difficulties in eluting IOR in the hydrophobic interaction step, which led to complete loss of protein. A careful reconsideration of the purification protocol was therefore necessary. Firstly, a procedure omitting both the heat precipitation and hydrophobic interaction steps was tried, leaving only the cation-exchange and size-exclusion chromatography steps after cell lysis. This worked for freshly grown cells, but after storage of the cells at 193 K the cation-exchange step did not retain the protein. A procedure was then tried that involved heat precipitation, a cation-exchange step and size-exclusion chromatography. However, the retention problem reoccurred at the first cation-exchange procedure. The retention problems during the cation-exchange step and the increased affinity in the hydrophobic interaction step were assumed to be a consequence of the high hydrophobicity of IOR, which causes it to interact with the (charged) lipids present in the cell lysate. The protein–lipid complexes that are expected to form have altered electrostatic properties and may not have affinity for the cation-exchange resin. We hypothesized that binding competition of a non-ionic detergent with the charged lipids might result in protein–lipid complexes with electrostatic behaviour similar to that of the unbound protein and restore protein affinity for the cation-exchange resin. To test this hypothesis, Triton X-100, a strong non-ionic detergent, was added to the cell lysate. A white flaky precipitation was observed and a clear red–brown supernatant solution was obtained after centrifugation. After applying the supernatant to the SQ Sepharose column, IOR was found to bind to the cation resin. A second cation-exchange step using a high-resolution Resource S column was used to compensate for the effect of the omission of the heat precipitation and HIC steps on the purity of the final sample. Using this procedure, the yield was 4%. However, the specific activity decreased from 13.9 units mg<sup>−1</sup> as determined by Lehmann to 8.1 units mg<sup>−1</sup>. Although the reason for this difference is not clear, it might be caused by a loss of the Mo atom as is often observed in other molybdopterin-

**Table 1**  
Summary of data sets measured.

Values in parentheses are for the highest resolution shell.

	Native	As peak	Fe peak	Fe inflection point
Wavelength (Å)	0.976	1.0450	1.7352	1.7415
Temperature (K)	100	100	100	100
Crystal data				
Space group	<i>P</i> 2 <sub>1</sub> 2 <sub>1</sub> 2 <sub>1</sub>			
Unit-cell parameters (Å)				
<i>a</i>	67.3	67.1	66.5	66.5
<i>b</i>	122.2	117.0	114.7	114.7
<i>c</i>	239.1	238.1	237.5	237.5
Mosaicity	0.9	0.31	0.26	0.26
Data collection				
Resolution (Å)	25–2.6 (2.66–2.60)	25–2.9 (3.0–2.9)	20–3.13 (3.32–3.19)	20–3.3 (3.4–3.3)
No. observations	1234059	306704	231175	399048
No. unique reflections	59051	80049	60990	52462
<i>R</i> <sub>merge</sub> † (%)	11.7 (37.8)	8.5 (34.0)	12.2 (39.8)	13.5 (41)
Completeness (%)	95.8 (93.7)	99.7 (100)	99.6 (100)	99.5 (100)
<i>I</i> / <i>σ</i> ( <i>I</i> )	5.1 (1.7)	12.1 (4.5)	10.4 (3.8)	13.4 (5.1)

$$\dagger R_{\text{merge}} = \frac{\sum_h \sum_i |I_{hi} - \langle I_h \rangle|}{\sum_h \sum_i I_{hi}}$$

containing enzymes (Rebelo *et al.*, 2000). The purity of the sample using the procedure described above is comparable to that reported earlier.

The purified protein produced crystals which appeared after 1 or 2 d and reached maximum dimensions after one week. However, spontaneous crystal growth using buffer *A* only occurred when crystallizing the protein directly after purification. After freezing and thawing the protein sample once, crystal growth had to be induced using (for example) streak-seeding. Crystal growth was more reproducible with PEG 8K (buffers *B1* and *B2*) crystallization buffers. However, seeding techniques were found to increase the definition of the crystals edges and were therefore applied for all crystallization experiments. Initial freezing trials of the crystals resulted in poorly diffracting crystals with highly anisotropic diffraction spots exhibiting poorly resolved reflections. Extensive trials of different cryoprotectants for both crystallization conditions did not improve diffraction to an acceptable level. Crystals were mounted in capillaries either using the harvesting buffer or a cryoprotectant solution. In both cases, the crystals did not diffract beyond 3.5–3.0 Å on an in-house rotating-anode generator. In contrast, freezing the crystals, both in the cryostream as well as in bulk liquid nitrogen, decreased the diffraction and increased the mosaicity and anisotropy to such an extent that useful data could not be obtained. Cross-linking (with glutaraldehyde or betaine monohydrate) proved to be necessary in order to stabilize the crystals upon freezing, which increased the reproducibility of the mounting process and resulted in diffraction comparable with that of crystals mounted in capillaries.

Crystals grown in crystallization buffer *A* belong to space group *P*2<sub>1</sub>2<sub>1</sub>2<sub>1</sub>, with unit-cell parameters *a* = 67.3, *b* = 122.2, *c* = 239.1 Å, while crystals grown in buffer *B2* have unit-cell parameters *a* = 66.5, *b* = 114.7, *c* = 237.5 Å (Table 1). The BaCl<sub>2</sub> in buffer *B2* has an impact on the *b* unit-cell parameter, which changes from 122.2 to 114.7 Å, a 6% decrease. This suggests a change in packing and concomitantly indicates non-isomorphism between crystals grown under the two different conditions. For both types of crystals, the Matthews coefficient is 2.4 Å<sup>3</sup> Da<sup>−1</sup> and the solvent content is 49% assuming the presence of two molecules in the asymmetric unit. In the self-rotation function, however, only peaks corresponding to space-group symmetry are observed (see below).

Although the sequence of IOR has low homology with other proteins of the XDH family, its overall fold is expected to be similar

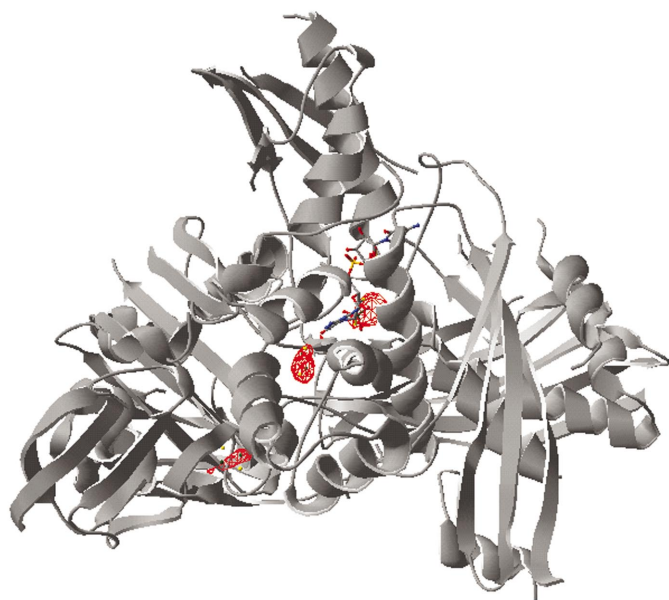


**Figure 2**

Anomalous electron-density map in the asymmetric unit contoured at  $3.5\sigma$  in red, calculated using *PHASER* phases combined with the anomalous difference of the Bijvoet pairs of the data set measured at the absorption peak of As. The model shown is MOP. The Mo active site and the two [2Fe-2S] clusters are shown as ball-and-stick representations and appear sequentially from the middle of the picture to the bottom left.

to that found for other members of the family. This is based on the observation that domain *A* has been relocated in the primary sequence, but can be expected to appear in approximately the same region in space in the three-dimensional structure. Molecular replacement was therefore attempted using four structures of members of the XDH family (*i.e.* XDH from bovine milk CODH, QOR and MOP) as search models. The structures were stripped of water molecules and superposed using the DALI server (Holm & Sander, 1993), after which parts with low structural similarity were removed from the models by manual inspection. Extensive molecular-replacement calculations using different models in a variety of programs did not result in a usable set of starting phases. The molecular-replacement algorithm in *PHASER* (Storoni *et al.*, 2004) using all four models did yield a clear solution and indicated the presence of two molecules in the asymmetric unit. The non-crystallographic symmetry element relating the two molecules is a twofold rotation axis parallel to the *c* axis of the unit cell and therefore parallel to the twofold crystallographic screw axis, which explains why no additional peaks are observed in the self-rotation function. Density-modification calculations using the program *DM* from the *CCP4* program package (Collaborative Computational Project, Number 4, 1994), starting from phases from *PHASER* and including non-crystallographic symmetry derived from the two molecules gave a clear solvent/protein boundary. Combination of the phases from *DM* and the anomalous signal measured at the wavelength of the arsenite absorption *K* edge of the arsenite-inhibited enzyme resulted in the anomalous maps shown in Fig. 2. A  $14\sigma$  peak appears close to the molybdenum site similarly located to that found in an analogously inhibited form of MOP that we have analyzed by crystallography (Boer *et al.*, 2004). In addition, anomalous density appears on the Fe atoms of the two [2Fe-2S] clusters. Clearly, an initial set of phases has been obtained that is essentially correct, but the resulting electron-density maps are not of sufficient quality to assign amino-acid residues along the backbone. Improvement of the

maps can be expected by including the anomalous differences of data sets measured at the As and Fe absorption edges.

In conclusion, we have found that applying the non-ionic detergent Triton X-100 in a precipitation step overcomes retention problems of IOR in the cation-exchange purification step. The purified protein was crystallized and initial diffraction experiments have been performed using PEG 4K as cryoprotectant in conjunction with cross-linking of the crystals. Native and anomalous data have been collected, which were used to obtain a molecular-replacement solution and to validate the initial set of phases obtained. Our efforts are now aimed at improving the phases and interpreting the electron-density map, which includes the use of the anomalous data in the density-modification calculations.

We thank the EU for funding (HRRN-CT-1999-00084). We thank Alice Pereira, Cristina Timóteo and Sergey Bursakov for helpful suggestions regarding purification and Shabir Najmudin for careful reading of the manuscript. We thank Mr Tony Page for growing the *B. diminuta* cells. DJL was supported by the BBSRC Core Strategic Grant to the John Innes Centre.

## References

- Boer, D. R., Thapper, A., Brondino, C. D., Romao, M. J. & Moura, J. J. (2004). *J. Am. Chem. Soc.* **126**, 8614–8615.
- Bonin, I., Martins, B. M., Purvanov, V., Fetzner, S., Huber, R. & Dobbek, H. (2004). *Structure*, **12**, 1425–1435.
- Bordas, J., Bray, R. C., Garner, C. D., Gutteridge, S. & Hasnain, S. S. (1979). *J. Inorg. Biochem.* **11**, 181–186.
- Canne, C., Lowe, D. J., Fetzner, S., Adams, B., Smith, A. T., Kappl, R., Bray, R. C. & Hüttermann, J. (1999). *Biochemistry*, **38**, 14077–14087.
- Collaborative Computational Project, Number 4 (1994). *Acta Cryst.* **D50**, 760–763.
- Cramer, S. P., Moura, J. J., Xavier, A. V. & LeGall, J. (1984). *J. Inorg. Biochem.* **20**, 275–280.
- Dobbek, H., Gremer, L., Kiefersauer, R., Huber, R. & Meyer, O. (2002). *Proc. Natl Acad. Sci. USA*, **99**, 15971–15976.
- Dobbek, H., Gremer, L., Meyer, O. & Huber, R. (1999). *Proc. Natl Acad. Sci. USA*, **96**, 8884–8889.
- Enroth, C., Eger, B. T., Okamoto, K., Nishino, T. & Pai, E. F. (2000). *Proc. Natl Acad. Sci. USA*, **97**, 10723–10728.
- Harrison, R. (2002). *Free Radic. Biol. Med.* **33**, 774–797.
- Hille, R. (1996). *Chem. Rev.* **96**, 2757–2816.
- Holm, L. & Sander, C. (1993). *J. Mol. Biol.* **233**, 123–138.
- Huber, R., Hof, P., Duarte, R. O., Moura, J. J., Moura, I., Liu, M. Y., LeGall, J., Hille, R., Archer, M. & Romao, M. J. (1996). *Proc. Natl Acad. Sci. USA*, **93**, 8846–8851.
- Kabsch, W. (1993). *J. Appl. Cryst.* **26**, 795–800.
- Lehmann, M., Tshisuaka, B., Fetzner, S. & Lingens, F. (1995). *J. Biol. Chem.* **270**, 14420–14429.
- Lehmann, M., Tshisuaka, B., Fetzner, S., Roger, P. & Lingens, F. (1994). *J. Biol. Chem.* **269**, 11254–11260.
- Lowry, O. H., Rosebrough, N. J., Farr, A. L. & Randall, R. J. (1951). *J. Biol. Chem.* **193**, 265–275.
- Monu, J. U. & Pope, T. L. Jr (2004). *Radiol. Clin. North. Am.* **42**, 169–184.
- Okamoto, K., Matsumoto, K., Hille, R., Eger, B. T., Pai, E. F. & Nishino, T. (2004). *Proc. Natl Acad. Sci. USA*, **101**, 7931–7936.
- Otwinowski, S. & Minor, W. (1997). *Methods Enzymol.* **276**, 307–326.
- Rebelo, J. M., Dias, J. M., Huber, R., Moura, J. J. & Romao, M. J. (2001). *J. Biol. Inorg. Chem.* **6**, 791–800.
- Rebelo, J. M., Macieira, S., Dias, J. M., Huber, R., Ascenso, C. S., Rusnak, F., Moura, J. J., Moura, I. & Romao, M. J. (2000). *J. Mol. Biol.* **297**, 135–146.
- Romao, M. J., Archer, M., Moura, I., Moura, J. J., LeGall, J., Engh, R., Schneider, M., Hof, P. & Huber, R. (1995). *Science*, **270**, 1170–1176.
- Schägger, H. & von Jagow, G. (1987). *Anal. Biochem.* **166**, 368–379.
- Storoni, L. C., McCoy, A. J. & Read, R. J. (2004). *Acta Cryst.* **D60**, 432–438.
- Truglio, J. J., Theis, K., Leimkuhler, S., Rappa, R., Rajagopalan, K. V. & Kisker, C. (2002). *Structure*, **10**, 115–125.